Applied Energy 140 (2015) 75–84

Contents lists available at ScienceDirect

Applied Energy

journal homepage: www.elsevier.com/locate/apenergy

Experimental study of occupancy-based control of HVAC zones ☆

Siddharth Goyal [a,*], Prabir Barooah [a], Timothy Middelkoop [b]

[a] Department of Mechanical and Aerospace Engineering, University of Florida, Gainesville, FL 32611, USA
[b] University of Missouri, Columbia, MO 65211, USA

HIGHLIGHTS

- Investigates performance of occupancy-based controllers through experiments.
- Experiments are performed for a single zone in a commercial building.
- High energy-savings are possible with only occupancy measurements.
- Feedback controller performs as well as optimal controller.
- Motion sensors can be effectively used for occupancy-based control in small zones.

ARTICLE INFO

Article history:
Received 13 March 2014
Received in revised form 25 November 2014
Accepted 27 November 2014

Keywords:
Occupancy based building climate control
Real-time experiments
VAV box control
Model predictive control
Energy-efficient buildings
Building thermal dynamics

ABSTRACT

We present experimental evaluation of two occupancy-based control strategies for HVAC (heating, ventilation, and air-conditioning) systems in commercial buildings that were proposed in our earlier simulation work. We implement these strategies in a test-zone of Pugh Hall at the University of Florida campus. By comparing their performance against a conventional baseline controller (that does not use real-time occupancy measurements) on days when exogenous inputs—such as weather—are similar, we establish the energy savings potential for each of these strategies. The two control strategies are of vastly different complexity: one is a rule-based feedback controller while the other is based on MPC (model predictive control) that requires real-time optimization based on dynamic models. The results of the evaluation are consistent with those of our prior simulation work, that (i) both occupancy based controllers yield substantial energy savings over the baseline controller without sacrificing thermal comfort and indoor air quality, and (ii) the much higher complexity MPC controller yields negligible benefit over the simple rule-based feedback controller. The experimental evaluation provides further confidence that high degree of energy savings is possible with simple control algorithms that use real-time occupancy measurements.

1. Introduction

Due to the large share of building sector in the energy consumption of the developed world, there is an increasing interest in energy efficiency, in particular, in reducing energy use of heating, ventilation and air-conditioning (HVAC) systems through advanced control methods [1–3].

In our previous study [1], we proposed occupancy-based control algorithms for energy-efficient control of HVAC systems and studied their performance through simulations. In this study we evaluate their performance through experiments in a single zone of a commercial building at the University of Florida campus.

The focus of our work is "zone-level control" of variable air volume (VAV) systems. VAV systems serve 30% of the U.S. commercial building floor area [4]. Fig. 1 shows a schematic of VAV HVAC system in a multi-zone commercial building. The control inputs (i.e., commands) that need to be determined are the (i) SA (supply air) flow rate and (ii) SA temperature at each VAV box. The controller does not affect variables such as CA (conditioned air) temperature and return air ratio that are varied at the Air Handling Units (AHUs).

Three control algorithms were tested through simulations in our earlier work [1] against a baseline controller: a simple rule-based controller called MOBS (Measured Occupancy Based Setback) that uses real-time occupancy measurements, a MPC (model predictive control)-based controller that uses measured occupancy

☆ This work has been supported by the National Science Foundation by Grants CNS-0931885 and ECCS-0955023.

* Corresponding author.
E-mail addresses: siddelec@gmail.com (S. Goyal), pbarooah@ufl.edu (P. Barooah), middelkoopt@missouri.edu (T. Middelkoop).

http://dx.doi.org/10.1016/j.apenergy.2014.11.064
0306-2619/

as a surrogate for occupancy predictions, and an MPC-based controller that has access to perfect (error-free) occupancy predictions for the future. The third one is of course not possible to implement in reality, but was tested in simulation to examine the best possible performance of an MPC strategy. The baseline control strategy they were compared against was the so-called "dual-maximum" controller that only uses temperature feedback but does not use occupancy information [1]. The conclusions drawn from the study were that (i) a significant amount of energy can be saved without sacrificing thermal comfort and IAQ (indoor air quality) by using real-time occupancy measurements, (ii) the rule-based feedback controller MOBS performs as well as MPC in terms of energy savings when both of them use occupancy measurements, and (iii) even when perfect occupancy predictions are available, MPC does not lead to significantly larger savings over the case when only occupancy measurements are available. The reason turned out to be ASHRAE ventilation standard 62.1-2010 [5], which requires a non-zero amount of outside air even during unoccupied periods for office-type buildings. The amount required during unoccupied times is a substantial portion of the outside air required during occupied times, which precludes the controller from reducing airflow drastically even when future occupancy is known to be 0 with certainty. An independent study [6] also arrived at a conclusion similar to (ii).

Since the conclusions in our previous study were drawn from simulations, they were necessarily dependent on the accuracy of the model used in the simulations. Obtaining an accurate model of building thermal dynamics is a challenging problem; see [7,8] and references therein for the extensive literature on this topic. In addition, the MPC formulations did not have any plant-model mismatch, i.e., the MPC controller had exact knowledge of the building dynamics in the simulation studies. In practical implementation, this is never the case. The main goal of the experimental evaluations reported here to determine how accurate the conclusions from [1] are in reality. Since occupancy measurements were identified to be crucial for the controllers in [1], another goal was to test robustness of the control schemes to imprecise occupancy measurements. It should be noted that we use the word occupancy to mean the number of occupants, which are difficult to obtain using inexpensive commercially available sensors. In the experiments, we estimated occupancy from binary PIR sensor measurements based on the zone size.

It turns out that the conclusions from the experimental evaluation are remarkably similar to those obtained during our prior simulation study [1], in spite of the many differences between a simulation model and a real building. In short, experiments verified the conclusions drawn from simulations, that (i) both occupancy-based controllers yield substantial energy savings over the baseline controller, and (ii) the much higher complexity MPC controller yields negligible benefit over the simple rule based feedback controller. Measurements of temperature, humidity, and CO_2 levels show that the energy savings were obtained without any reduction in occupants' thermal comfort or IAQ. The experiments also showed that the controllers are robust to the inaccuracies introduced by the motion-detection based occupancy estimation scheme used.

1.1. Contribution over related work

Since the focus of this paper is experimental evaluation of occupancy based controllers, we limit the discussion here to papers that present experimental results of control strategies that use occupancy information. For a review of literature on simulation-based work, the interested reader may consult our previous study [1] and references therein. We classify prior work in two categories: MPC-based algorithms and RBC (rule-based control) algorithms. The references [9,2,10–12] belong to the former while [13–17] belong to the latter. The energy savings reported in prior work are shown in Table 1.

There is a great variety of approaches within the rule based controllers implemented by various researchers. The controller proposed by Balaji et al. [13] detects presence/absence from PIR and door sensors to turn on/off the HVAC system. In another study done by Balaji et al. [14], Wi-Fi signatures of smartphones are used to detect whether the rooms are occupied. The controller changes the cooling and heating set points during unoccupied times [14]. The controller proposed by Gao and Keshav [15] uses Kinect® to detect presence/absence in the room, and changes the threshold of thermal comfort during unoccupied times. Padmanabh et al. [16] propose a method for energy-efficient HVAC control in conference rooms through the use of sound and light sensors. By putting a threshold on the measurements obtained from the light and sound sensors, the controller decides whether the room is unoccupied and turns off the HVAC system and lights during the unoccupied time. The controller proposed by Erickson et al. [17] changes the ventilation rate and set point of room temperature based on the occupancy measurements and predictions. Occupancy estimates are obtained using data from a PIR sensor and a camera with predictions from a model using a particle filter.

The MPC controller proposed by Dong et al. [9] uses temperature, CO_2, humidity, acoustics, light, and motion sensors to predict occupancy through Markov Models. The controller sets back the

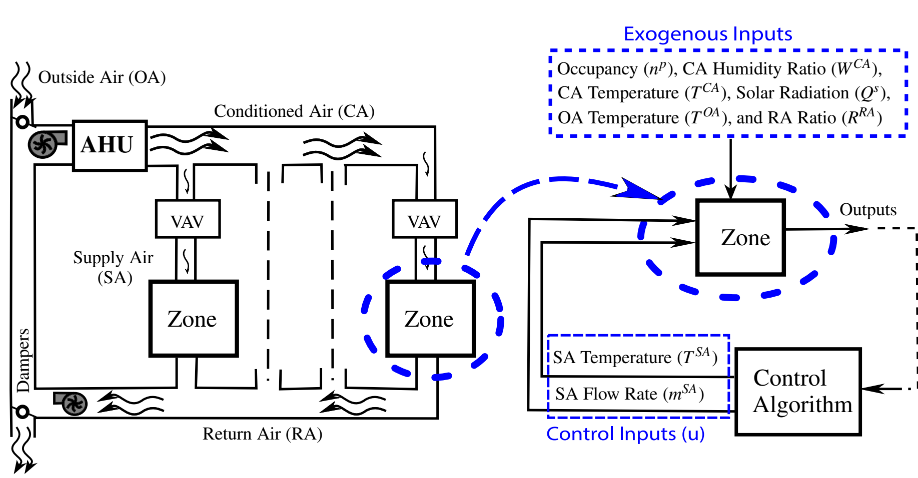

Fig. 1. Generic scheme for the implementation of a zone-level control algorithm for a VAV HVAC system.

Table 1
Energy savings in percentage reported in earlier work.

MPC					RBC				
[9]	[2]	[10]	[11]	[12]	[13]	[14]	[15]	[16]	[17]
17–30	15–28	30–70	N/A	12–42	9–16	17	25	13	30

zone temperature during times it predicts the zone to be unoccupied. The MPC controller proposed by Siroky et al. [2] reduces the desired room temperature during nights and weekends to save on heating energy by utilizing thermal inertia of the building. The MPC scheme tested in [12] controlled both zone commands (temperature of zone discharge air) and AHU commands (hot and cold deck temperature, flow rate) based on forecasts of thermal loads. The controller sought to maintain temperature in each zone within a tight bound around the thermostat value, but ventilation constraints were not explicitly considered.

Prior work did not report the effect of their control strategies on IAQ and humidity. While humidity and temperature together determine thermal comfort according to ASHRAE guidelines [18], only indoor temperature is reported. We provide measurements of humidity and CO_2 apart from temperature. These measurements show that both thermal comfort and IAQ are not compromised by our controllers in the interest of energy efficiency.

Among the prior work, refs. [9,2] report results based on implementation for long periods of time (a few months), while the others base their energy saving estimates on results from one or a few days. However, only [12] accounted for the variations due to weather. Difference in weather can and does cause large changes in cooling and heating energy use even without a change in the control strategy. The sensitivity of estimated savings to changes in weather are particularly severe if the time duration of the control experiments is short. Even in [12], weather-related variation was addressed by using "...data for days when ambient, as well as indoor conditions, were similar ...", without clarifying how to measure such similarity. In this paper we present a formal method for identifying the "best" days for comparing the performance of distinct controllers.

Earlier work has compared either MPC with conventional controllers [9,2,10,11] or rule-based feedback controllers with conventional controllers [13–17]. No study has compared all three types of controllers together. However, since the cost of MPC implementation is substantially larger than that of a rule-based controller, it is imperative to determine what is the additional benefit obtained from that extra cost. Our previous study attempted to answer this question through simulations by comparing all three types of controllers together under similar conditions. This is precisely what the work presented here does, but though experiments in a real building.

To the best of our knowledge, only one prior study [12] has shown an MPC controller implementation on a VAV HVAC system. Such an implementation faces a number of challenges. First, it needs a calibrated dynamic model that can be used to prediction of thermal variables. We use a non-linear RC network model [19] for the thermal dynamics that includes both temperature and humidity dynamics. In HVAC systems with forced air circulation and dehumidification through a cooling coil, moist air enthalpy exchange—and therefore humidity—plays a key role in the thermal dynamics as well as occupant comfort. Incorporating humidity dynamics in the model makes the model non-linear, which introduces non-convex constraints in the optimization problem solved by the MPC controller. Second, the cost function we use during on-line optimization in MPC is the most natural one: total energy consumption over the optimization horizon, which includes cooling, reheating, and mechanical (fan) energy. This cost function is non-convex in the decision variables. Coupled with the non-linear dynamics, which leads to non-convex constraints, the overall optimization problem becomes a non-convex problem. Third, real-time computation constraints bring further challenges. Here "real-time computation" means computations have to be completed in a much shorter time compared to the time interval at which control commands are updated. Due to non-convexity, the optimizer in MPC may either fail to converge to a local optimal solution within the allowed time or fail to converge to a highly sub-optimal solution that may in fact be less energy-efficient than a baseline controller. In addition, a state-observer needs to be implemented to estimate the state of the dynamic model from the observations since the model has more states than what can be measured. Due to the non-linear nature of the dynamic model, an EKF (extended Kalman filter) was used. Unlike the linear counterpart (KF), the EKF does not come with a guaranteed stability, so that the state estimates can potentially diverge. Finally, the optimization problem may not be feasible. During real-time implementation, the controller needs to be able to handle these special cases. The implemented controller was therefore a hybrid between MPC and rule-based controllers, where the rules become active when the optimizer fails to provide a "good" solution. In contrast, all previously mentioned work on MPC used a convex optimization problem formulation through quadratic cost function and linear dynamic constraints, making implementation considerably simpler, but with possible loss of model accuracy.

1.2. Organization of the paper

The rest of the paper is organized as follows. Section 2 briefly describes the zone-level control algorithms, which are implemented in real-time inside the zone of a building at the University of Florida Campus. The experimental setup, which includes the zone configurations, calibration/validation of the models used by the controllers, and selection of the controller design parameters, are presented in Section 3. Experimental results comparing the performance of the controllers are shown in Section 4. Section 5 concludes the results, discusses the potential impact of this study in selecting an appropriate controller for zone-level building HVAC control, and proposes ways to extend this work in future.

2. Control algorithms

In the interest of being self-contained, we briefly describe the two zone-level control algorithms, *MOBS* (Measured Occupancy Based Setback) and *MOBO* (Measured Occupancy Based Optimal), which were earlier proposed in [1]. For details the interested reader is referred to [1].

The outputs, i.e., actuation signals, of all three controllers are the same: (i) flow rate and (ii) temperature, of air supplied to the zone. The commanded set points are maintained by lower level PI controllers. The VAV terminal box can only increase the temperature of the air by using a reheat valve, but cannot decrease it beyond the AHU discharge air temperature.

2.1. Measured Occupancy Based Setback (MOBS) Controller

The *MOBS* controller is a combination of the dual maximum [20, Chapter 47] and occupancy based feedback, which requires occupancy (n^p) measurements and zone temperature (T_z) measurements. In this strategy, the control logic is divided into four modes based on the zone temperature: (i) Re-heating (ii) Heating (iii) Dead-Band and (iv) Cooling, which are shown schematically in Fig. 2.

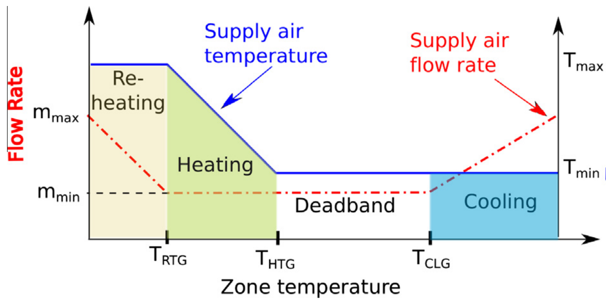

Fig. 2. Schematic representation of the baseline control strategy ("dual maximum").

The re-heating mode is turned on if the zone temperature stays below the "Re-heating Set-Point (RTG)" for more than 10 min. Similarly, the cooling mode is turned on if the zone temperature remains above the "Cooling Set-Point (CLG)" for more than 10 minutes. The heating mode is turned on if the zone temperature stays between RTG and "Heating Set-Point (HTG)" for more than 10 minutes. The dead-band mode is turned on if the zone temperature stays between HTG and CLG for more than 10 minutes. In the re-heating mode, the temperature of supply air is set to maximum possible value $\left(T^{SA}_{high}\right)$, and the flow rate of supply air is varied using a PID controller to maintain the zone temperature to a desired set-point T^{set}. In the heating mode, the supply air flow rate is set to the minimum allowed value, and the temperature of supply air is controlled by a PID controller so that the zone temperature is maintained close to the set-point (T^{set}). The minimum allowed value for the flow rate at time t is determined as follows:

$$\text{Minimum Allowed Flow Rate at time } t = m^{SA}_p(t)n^p(t) + \alpha m^{SA}_{low}(t),$$
$$\text{where } m^{SA}_p(t) = \frac{m^{OA}_p}{1 - R^{RA}(t)}, \quad m^{SA}_{low}(t) = \frac{m^A_z A_z}{1 - R^{RA}(t)}, \tag{1}$$

where A_z denotes the zone floor area, $n^p(t)$ and $R^{RA}(t)$ represent the occupancy and return air ratio, respectively, measured at time t. Constants m^{OA}_p and m^A_z denote the minimum outside air requirements per person and per floor area, respectively, in that zone. The IAQ factor of safety is denoted by α. When $\alpha = 1$, these calculations yield the minimum airflow requirements specified by ASHRAE ventilation standard 62.1-2010 [5]. In the dead-band mode, no re-heating is performed, i.e., $T^{SA} = T^{CA}$, and supply air flow rate is set to the minimum allowed value (1). In the cooling mode, no heating or re-heating is performed, i.e., $T^{SA} = T^{CA}$, but the flow rate of supply air is varied to maintain the desired set-point T^{set} in the zone.

Note that the temperature set-points during all the modes are determined based on whether the zone is occupied or not:

$$\left.\begin{aligned} RTG(t) &= T^{unocc}_{RTG} \\ HTG(t) &= T^{unocc}_{low} \\ CTG(t) &= T^{unocc}_{high} \end{aligned}\right\} \text{ if } n^p(t) = 0, \quad \left.\begin{aligned} RTG(t) &= T^{occ}_{RTG} \\ HTG(t) &= T^{occ}_{low} \\ CTG(t) &= T^{occ}_{high} \end{aligned}\right\} \text{ if } n^p(t) \neq 0. \tag{2}$$

The choice of design variables $T^{unocc}_{RTG}, T^{occ}_{RTG}, T^{unocc}_{low}, T^{occ}_{low}, T^{unocc}_{high}, T^{occ}_{high}$ involves a trade-off between energy savings and thermal comfort; see [1] for a detailed discussion on the choice of design variables.

2.2. Measured Occupancy Based Optimal (MOBO) Controller

The *MOBO* controller is an MPC-based control algorithm. The block diagram of the implementation of the *MOBO* controller is shown in Fig. 3. Time is measured with a discrete index $k = 0, 1, \ldots$, where the time period between k and $k+1$ is denoted by Δt. The *MOBO* controller computes the control inputs $(u(k) = T^{SA}(k), m^{SA}(k))$ over K time indices by solving an optimization

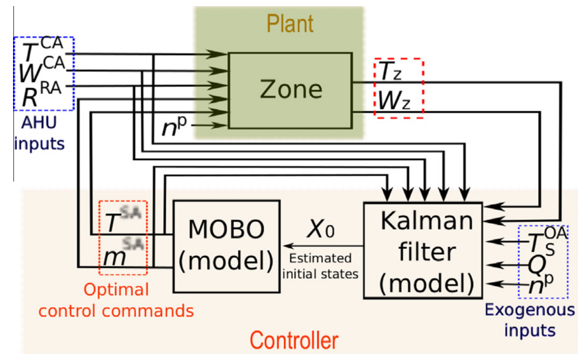

Fig. 3. Schematic representation of the implementation of *MOBO* controller.

problem, which minimizes total energy consumption over that period while maintaining thermal comfort and IAQ. The control inputs are applied at the current time index k, and the optimization problem is solved again at time index $k+1$ to compute the control inputs for the next K time steps. The whole process is repeated at the $(k+1)$-th time index.

To solve the underlying optimization problem, *MOBO* needs (i) a model of the zone hygro-thermal dynamics, (ii) initial state of the hygro-thermal dynamics model, and (iii) predictions of the exogenous inputs such as T^{OA}, W^{OA}, Q^s and n^p, over the time horizon of optimization. Models of the zone hygro-thermal dynamics and power are the same as previously described in [19,1], respectively. An EKF (extended Kalman filter)-based state observer is used to estimate the initial state of the model at the start of the optimization. The linear part of the original 14 state model for a single zone (13 states for the zone temperature and the temperature interior to the walls, and 1 state for humidity ratio) is non-observable, we have reduced the model order using a non-linear balanced truncation scheme [19]. The reduced order model has 8 states, which has an observable linear part. The predictions of exogenous inputs T^{OA}, W^{OA}, and Q^s are assumed available from weather forecasts. We assume that the predicted occupancy for the next K time indices is same as the measured occupancy at the k-th time period: $n^p(i) = n^p(k), i \geqslant k$. Based on the occupancy measurements, we divide the control logic into two modes: (i) Occupied and (ii) Unoccupied, which are briefly explained.

Occupied mode: The controller operates in the occupied mode if the zone is occupied at the k-th time index, i.e., the measured occupancy at the beginning of the time interval $[k\Delta t, (k+1)\Delta t]$ is at least 1. The optimal control inputs for the next K time indices are computed by solving the following optimization problem:

$$U^\star := \underset{U}{\operatorname{argmin}} G(U), \tag{3}$$

where $U = [u(k)^T, \ldots, u^T(k+K)]^T \in \mathbb{R}^{2(K+1)}$ and $G(U) = \sum_{i=k}^{k+K} E(i)$, subject to the following constraints:

$$\left.\begin{aligned} &T^{occ}_{low} \leqslant T_z(i) \leqslant T^{occ}_{high}, \\ &W^{occ}_{low} \leqslant W_z(i) \leqslant W^{occ}_{high}, \\ &T^{CA} \leqslant T^{SA}(i) \leqslant T^{SA}_{high} \\ &m^{SA}_p n^p(i) + \alpha m^{SA}_{low} \leqslant m^{SA}(i) \leqslant m^{SA}_{high} \end{aligned}\right\} \forall i = k, \ldots, k+K, \tag{4}$$

where E represents the total energy consumption.

Unoccupied mode: The controller operates in the unoccupied mode if the measured occupancy at the time index k, i.e., at the beginning of the k-th time period, is observed to be 0. At the k-th time index, the optimal control inputs for the next K time indices are obtained by solving the following optimization problem:

$$U^\star := \underset{U}{\operatorname{argmin}} G(U), \tag{5}$$

subject to the following constraints:

$$\left.\begin{array}{l} T_{low}^{unocc} \leqslant T_z(i) \leqslant T_{high}^{unocc} \\ W_{low}^{unocc} \leqslant W_z(i) \leqslant W_{high}^{unocc} \\ \alpha m_{low}^{SA} \leqslant m^{SA}(i) \leqslant m_{high}^{SA} \\ T^{CA} \leqslant T^{SA}(i) \leqslant T_{high}^{SA} \end{array}\right\} \forall i = k, \ldots, k+K. \tag{6}$$

The reason for these constraints are described in [1].

An energy related performance metric (*% Savings*), which is used to present the energy savings over the baseline controller, is defined as

$$\%\ \text{Savings} = \frac{E_{BC} - E_C}{E_{BC}}, \tag{7}$$

where E_C and E_{BC} are the energy consumed by the controller C and the baseline controller, respectively, over ΔT time period.

3. Experimental setup

Experiments are performed in a single room on the second floor of Pugh Hall at the University of Florida campus, Gainesville, FL, which is shown in Fig. 4. One terminal VAV box with reheat is solely dedicated to this room, making it an HVAC zone. Identity of the zone is not disclosed due to privacy reasons. We call this zone "test-zone". It is a typical small office, which has a North-facing window of area 2.8 m^2. The test-zone has three internal walls (Wall1, Wall2, and Wall3) and one external wall (Wall4), with dimensions of $4.4\ m \times 2.7\ m$, $4.4\ m \times 2.7\ m$, $4.8\ m \times 2.7\ m$, and $4.8\ m \times 2.7\ m$, respectively.

3.1. Comparison between controllers tested on distinct days

Comparison between distinct controllers tested on different days is difficult because external conditions (e.g., weather) and internal conditions (e.g., occupancy, conditioned air, etc.) can never be exactly the same. A method to measure the distance between two days has been proposed in [21], which can be used to identify pairs of days that have the minimum distance in terms of these external and internal variables. In this paper we extend this method to determine a "best" set of three days for comparison on which the three controllers (baseline, MOBS, and MOBO) were in operation.

Let $I = (i_1, i_2, i_3)$ be a set of three distinct days such that the following condition, which we denote by C1, is satisfied: day i_1 used the baseline controller, day i_2 used the MOBS controller and day i_3 used the MOBO controller, respectively. The function $\mu(I)$ defined below is a measure of similarity among the days in I:

$$\mu(I) := \int_0^1 \left[\left| h_{amb}^{i_1}(t) - h_{amb}^{i_2}(t) \right| + \left| h_{amb}^{i_2}(t) - h_{amb}^{i_3}(t) \right| + \left| h_{amb}^{i_3}(t) - h_{amb}^{i_1}(t) \right| + \right. \tag{8}$$

$$\left. \left| h_{CA}^{i_1}(t) - h_{CA}^{i_2}(t) \right| + \left| h_{CA}^{i_2}(t) - h_{CA}^{i_3}(t) \right| + \left| h_{CA}^{i_3}(t) - h_{CA}^{i_1}(t) \right| \right] dt, \tag{9}$$

where the subscript "*amb*" denotes the ambient air outside of the building, the subscript "*CA*" represents the conditioned air, $h^{(j)}(t)$ is the specific enthalpy of air at time t of the j-th day. Note that t has the unit of days, meaning $t = 0$ corresponds to 00:00 h and $t = 1$ corresponds to 24:00 h.

Let $\mathscr{I}$ be a set of triplets of days such that each element $I \in \mathscr{I}$ satisfies the condition C1. For every element in $\mathscr{I}$, the triple with the most similarity measure was identified by performing the following optimization through direct search:

$$I^* = \arg\min_{I \in \mathscr{I}} \mu(I). \tag{10}$$

The search set $\mathscr{I}$ was constructed to ensure similarity of internal conditions as well. This was done by making sure for every $I = (i_1, i_2, i_3)$, if i_1 is a working day, both i_2 and i_3 are working days, and all holidays/semester-breaks are excluded. The search set $\mathscr{I}$ was also limited by the number of days for which we had relevant measurements.

3.2. Measurements, computation, and actuation

Only a temperature sensor is pre-installed in the test-zone that is connected to the building automation system (BAS), since the baseline controller that usually operates the VAV box uses only temperature measurements. For the purpose of our experiments, we installed a wireless sensor node that provides measurements of humidity, CO_2, and occupant's presence through a PIR sensor. Fig. 5 shows pictures of such a sensor node. More details on the sensor node are available in [22].

Measurements of all four sensors in the node are transmitted wirelessly to a base station, which transmits the data from multiple nodes to a database hosted on a remote computer. A control computer reads the PIR sensor data from the database and space temperature measurements from the BAS, and computes the control commands. Since the PIR sensor only provided presence/absence of occupants but not the number of people, we scaled the binary measurements to an estimated occupancy by multiplying by three. This scaling was done due to two reasons. The test-zone is an office with a designed occupancy of two persons, so the chances of more than three people being present are small. In addition, even though most of the time only one occupant was present, by assuming presence of humans indicates the presence of three persons, a factor of safety was built against the controller commanding too little airflow rate, which could adversely affect IAQ.

Control computations were performed in MATLAB©. The MPC-based MOBO controller uses IPOPT [23] within a MATLAB© environment to solve the underlying optimization problem. Computed commands are executed on the VAV box by using a custom-built software platform, which was developed for both data acquisition from and control of HVAC equipment. We refer the interested reader to [24] for further details on the software architecture.

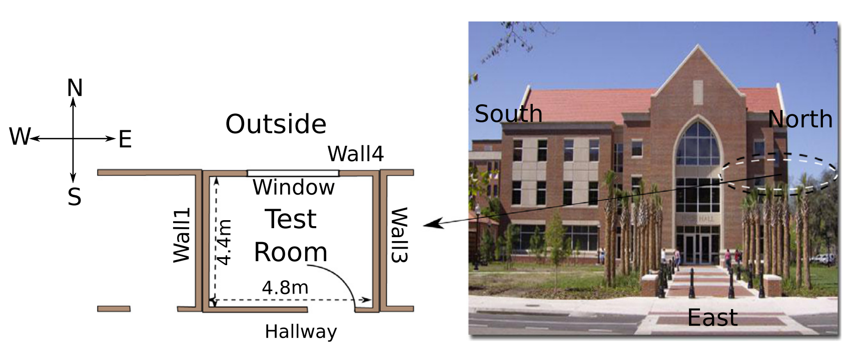

Fig. 4. Layout of the test-zone in Pugh Hall at the University of Florida campus, Gainesville, FL, USA.

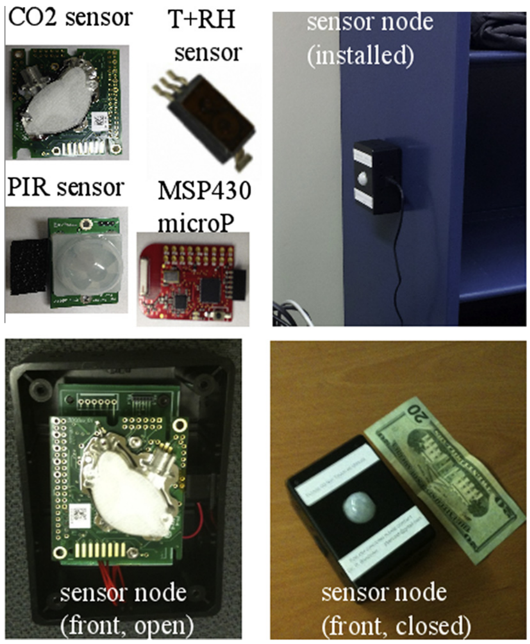

Fig. 5. Components of the wireless sensor node and an installed node in an office in Pugh Hall.

A non-linear RC network model with 13 states was used for predictions inside the MOBO controller. The structure of the model is described in [19]. The model is calibrated with data collected from the test-zone. The procedure and the tuned resistance and capacitance values of the walls and windows are explained in our earlier work [1]. Calibrated models of fan power, conditioning power at AHU, and reheating power at the terminal box are also the same as in [1].

The MPC-based controller also needs predictions of the surrounding space temperatures and weather (temperature and humidity), which serve as inputs to the test-zone model. The predictions of the surrounding space temperatures, outside temperature, and outside humidity are assumed same as their measurements at the current time. The surrounding spaces also have pre-installed temperature sensors which are obtained in real-time from the BAS. The measurements for the outside weather are obtained from the University of Florida Physics Department Weather Station [25]. The MPC controller uses these predictions as inputs to the hygro-thermal dynamics model of the test-zone to obtain predictions of the zone's temperature and humidity. Occupancy predictions for the time horizon of optimization in the MOBO controller were assumed to be the same as the current estimated occupancy.

3.3. Choice of parameters

The baseline controller in the Pugh Hall uses a nighttime setback in which the test-zone temperature is set to 22.8 °C from 6:30 a.m. to 10:30 p.m. and the zone temperature is set back to 21.1 °C during the time 10:30 p.m.–6:30 a.m. We could not find concrete information on the control logic used by the baseline controller at Pugh Hall to maintain the set-points. It seems from the data that the baseline controller uses the dual maximum strategy [20, Chapter 47]. The Minimum Allowed Flow Rate supplied by the VAV box in the test-zone is 0.05 kg/s (90 cfm). For the baseline controller, the maximum flow rate supplied by the VAV box in test-zone is 0.125 kg/s (220.0 cfm). Therefore, we choose the same maximum flow rate for the *MOBS* and *MOBO* controllers, i.e., $m^{SA}_{high} = 0.125$ kg/s (220.0 cfm). The baseline controller closes the outside air dampers at the AHU during the nighttime setback time period to reduce energy consumption, which leads to 100% return air ratio, i.e., $R^{RA} = 1$. However, if the *MOBS* and *MOBO* controllers choose $R^{RA} = 1$, the minimum flow rate calculated using (1) is infinite during that time. Therefore, the *MOBS* and *MOBO* controllers choose $R^{RA} = 0.7$ during the nighttime setback time period. This value of R^{RA} is used by the baseline controller during day time. The IAQ factor of safety is chosen as $\alpha = 1.1$, which is motivated by the assumption that the flow rate sensor errors are in the range of 10%. Other design parameters are shown in Table 2.

In Fig. 6, the comfort envelope specified in [26, Chapter 8] is shown in the striped black area, and the envelope chosen here during the occupied and unoccupied time is shown in dashed red and blue boxes, respectively. The comfort envelope is defined by the constraints on the test-zone temperature and humidity ratio. The constraints on the zone temperature and humidity ratio are chosen so that when they are met, the zone-climate meets the ASHRAE mandated conditions [26].

4. Experimental results

We performed experiments on several days for both the *MOBS* and *MOBO* controllers. We identify three days from the available dataset such that a distinct controller was operational in each of these three days, and the ambient conditions among all three days were closest, by using the method described in Section 3.1. The dataset used to select the closest days is shown Table 3. The three closest days are: Aug 6th, 2013 for the baseline controller; Aug 7th, 2013 for the MOBS controller; Aug 9th, 2013 for the MOBO controller, i.e., I^* = (6th Aug 2013, 7th Aug 2013, 9th Aug 2013). The value of similarity measure for the corresponding set (I^*) is 20.05, i.e., $\mu(I^*) = 20.05$. The values of similarity measure μ for the rest of triplet set ($\mathscr{I}$) are not shown due to space limit.

Fig. 7 shows the exogenous inputs during those three days. Fig. 7(a) and (b) shows the OA temperature and OA humidity ratio, respectively. Fig. 7(d) and (d) shows the CA temperature and CA relative humidity, respectively. The CA temperature increases during the nighttime setback period and its relative humidity decreases during that time, but is almost fully saturated (95% relative humidity) at 12.5 °C temperature for rest of the day. Fig. 7(f) shows that the test-zone is occupied for approximately 8 h during each of the three days/experiments.

Fig. 8 shows the control inputs (SA flow rate and temperature) and outputs (zone temperature, zone humidity, and zone CO_2 concentration) obtained by implementing the baseline, *MOBS*, and *MOBO* controllers.

4.1. Thermal comfort and IAQ

The main task of a climate control system is to maintain thermal comfort and IAQ; energy efficiency is a secondary goal. So

Table 2
Design parameter values used by the *MOBS* and *MOBO* controllers; the units in the parenthesis are associated with the corresponding values in the parenthesis.

Temperature parameters

T^{set} °C	T^{SA}_{high} °C	T^{unocc}_{RTG} °C	T^{occ}_{RTG} °C	T^{occ}_{low} °C	T^{occ}_{high} °C	T^{unocc}_{low} °C	T^{unocc}_{high} °C
22.8	30.0	20.9	21.8	21.9	23.6	21.1	24.4

Humidity and other parameters

W^{unocc}_{low} $\frac{g}{kg}$	W^{occ}_{low} $\frac{g}{kg}$	W^{unocc}_{high} $\frac{g}{kg}$	W^{occ}_{high} $\frac{g}{kg}$	K	Δt min	ΔT h	m^{OA}_{p} $\frac{kg}{s}$ (cfm)	m^{A}_{z} $\frac{kg}{sm^2}$ $\left(\frac{cfm}{m^2}\right)$
7.4	7.4	10	10	3	10	24	0.0028 (5.0)	0.0004 (0.65)

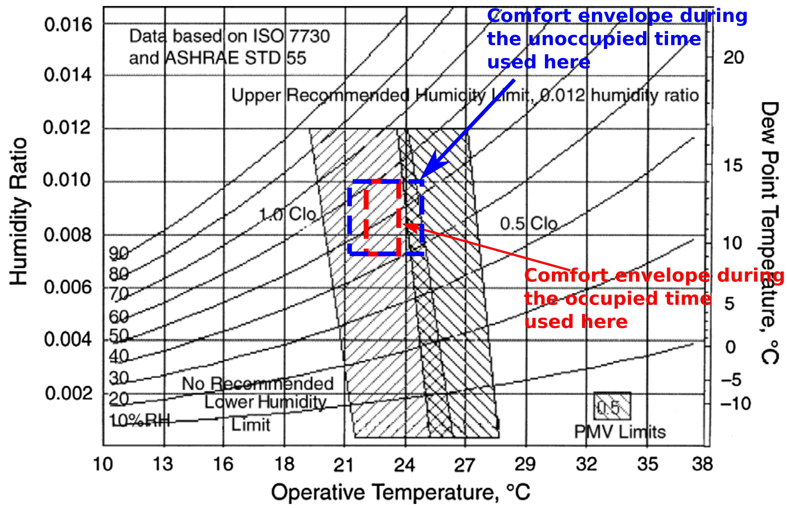

Fig. 6. Comfort envelope chosen for the occupied and unoccupied time periods during the experiments.

Table 3
Distinct days on which the control experiments were performed.

	Baseline	MOBS	MOBO
Days (Year 2013)	Jun 17, Jun 18, Jun 19, Jun 20, Jun 21, Jul 9, Jul 12, Jul 17, Aug 1, Aug 6	Jul 10, Jul 16, Aug 2, Aug 7	Jul 15, Jul 22, Aug 5, Aug 9

we discuss the effect of the controllers on comfort and air quality first.

Zone temperature: The temperature bounds on the zone temperature are represented by magenta colored lines in the zone temperature plots in Fig. 8. All the controllers are able to keep the zone temperature within the allowable bounds for most of the time. The bounds depend on whether the zone is occupied or not, which is determined from the PIR sensors. The baseline controller, of course, does not use this information.

As shown in the figure, the baseline controller maintains the zone temperature at a constant value of 22.8 °C during the day, and relaxing the bounds only during the nighttime setback period (10:30 p.m.–6:00 a.m.). However, the *MOBS* and *MOBO* controllers let the zone temperature float in wider range during both occupied and unoccupied times, particularly during the unoccupied times. With the *MOBS* and *MOBO* controllers, the zone temperature drops down to 21.2 °C during unoccupied times at night, which is a lower bound on the zone temperature for unoccupied times. When the zone gets occupied around 9:30 a.m., the zone temperatures increases to 22.9 °C, which is a lower bound on the zone temperature during occupied times.

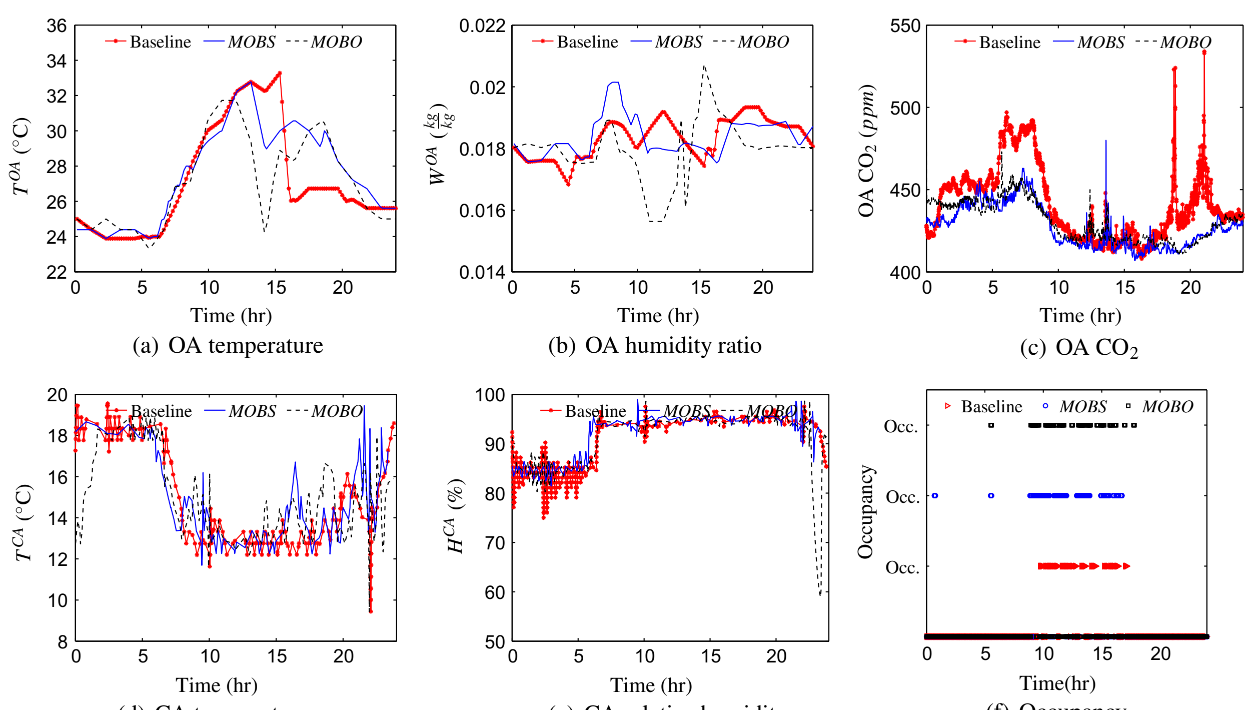

Fig. 7. Exogenous inputs: OA temperature, OA humidity ratio, OA CO_2 concentration, CA temperature, CA relative humidity, and occupancy over 24-h time period, used during the various controllers.

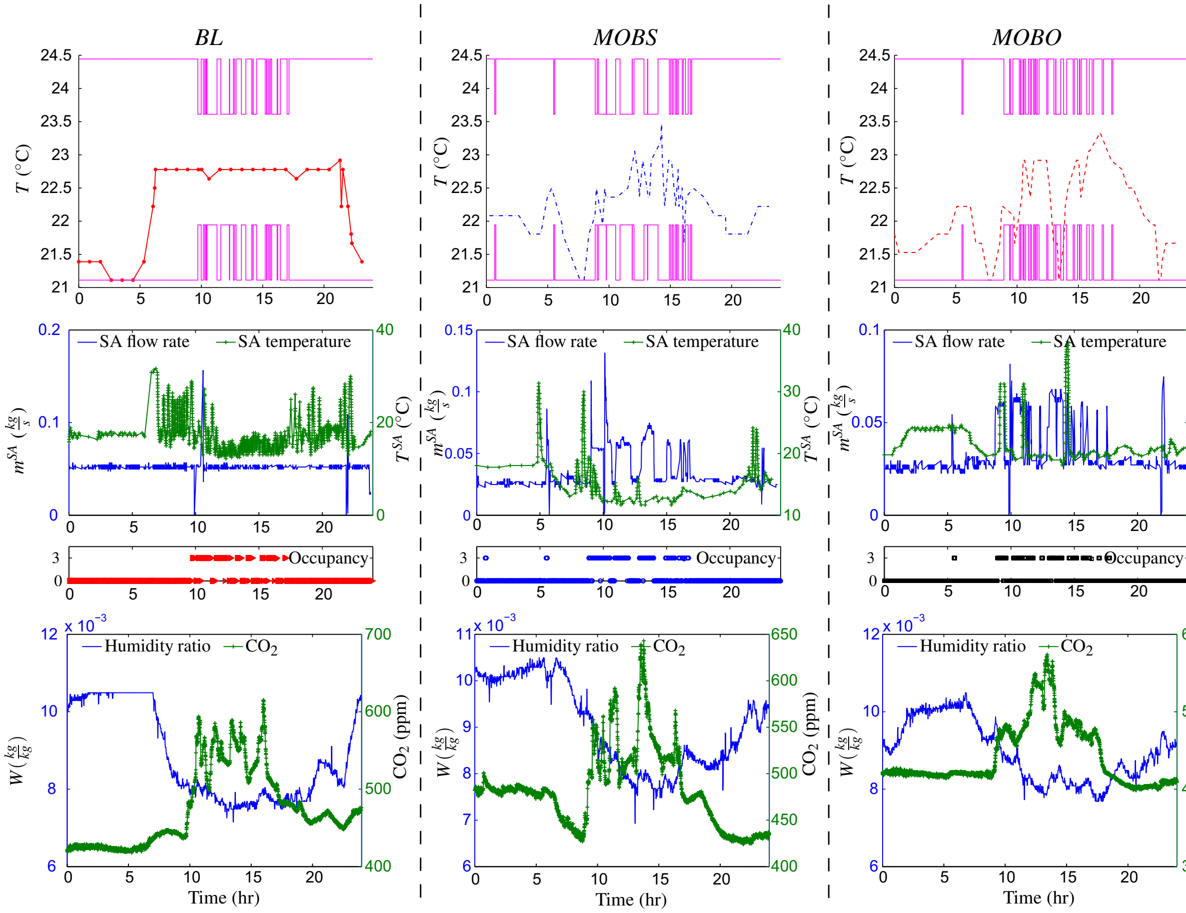

Fig. 8. Zone temperature, SA temperature, SA flow rate, zone humidity ratio, and zone humidity ratio during 24-h time period for various controllers. The figures in the left column correspond to the *BL* controller; the figures in the middle column correspond to the *MOBS* controller; the figures in the right column correspond to the *MOBO* controller.

Zone humidity: The zone humidity stays within the allowable range throughout the day for all the controllers. In fact the combined temperature-humidity values always fall inside the thermal comfort envelope as shown in Fig. 6. For all the controllers, the zone humidity from 10:30 p.m. to 6:00 a.m. is high, approximately 0.01 $\frac{\text{kg}}{\text{kg}}$, due to the high CA humidity ratio from the AHU. When the CA humidity ratio decreases around 6:30 a.m., the zone humidity ratio during the baseline control decreases at a faster rate than the rate at which the zone humidity decreases during the *MOBS* and *MOBO* controls. It occurs because the baseline controller supplies higher flow rates than the flow rates supplied by the *MOBS* and *MOBO* controllers during that time.

Zone CO_2 concentration: CO_2 concentration in the zone is less than 650 ppm throughout the day for all the three controllers. The CO_2 concentration during unoccupied times is lower than that of during the occupied times due to the CO_2 released by occupants.

Based on the temperature, humidity and CO_2 concentrations shown in Fig. 8, we can claim that thermal comfort and IAQ of the zone is maintained by all the controllers.

4.2. Energy consumption

The total energy consumption consists of fan energy to push the air, conditioning energy used by the cooling coils inside the AHU, and reheating energy used by the heating coils at the VAV box. These energy calculations are done using the calibrated power model described in [1]. The enthalpy calculations require the measurements of the zone temperature and humidity, SA flow rate and temperature, OA temperature and humidity, CA temperature and humidity, and return air ratio, all of which are measured during the experiments. The daily energy consumption during the baseline, *MOBS*, and *MOBO* controls are estimated to be 62.5 MJ, 38.0 MJ, and 37.7 MJ, respectively. The *MOBS* controller therefore results in 39% energy savings over the baseline controller. Almost the same energy savings (40%) are obtained by the *MOBO* controller over the baseline controller. The main contributors to the high energy savings obtained are: reduction of the flow rate during unoccupied times, and the relaxed temperature bounds during both occupied and unoccupied times—especially during unoccupied times—that reduce both flow rate and reheating.

4.3. Control inputs

SA flow rate: The baseline controller maintains a constant SA flow rate in the zone throughout the day. However, the *MOBS* and *MOBO* controllers reduce the SA flow rate during the unoccupied times, and increase the flow rates during the occupied times. We have noticed unexpected sudden peaks in the SA flow rate values twice a day around 10:00 a.m. and 10:30 p.m. These peaks are due to the change in the static pressure set-point at the AHU. We have also analyzed the SA flow rate values on several other days and observed similar peaks at the same time on these days as well.

SA temperature: During the baseline control, the SA temperature keeps on oscillating between its high and low values, especially from 6:30 a.m. to 11:00 a.m. This is because the SA flow rate is high and the air delivered from the AHU is cold, so periodic reheating is required to maintain a constant zone temperature of 22.8 °C. During the middle of the day this effect is less pronounced due to other sources of heat gain. In case of the *MOBS* and *MOBO* controls, the SA temperature increases only when the zone temperature is low and outside the allowable temperature range. Since these controllers supply a reduced flow rate during the unoccupied times, reheating is not required as often. As a result, the frequency of oscillations in the SA temperature during the *MOBS* and *MOBO* controls are lower than those during the baseline control. It is likely that smaller oscillations in the reheating will reduce mechanical wear and tear in the reheat valve. So the MOBS and MOBO controllers may have additional unintended benefits of increasing equipment life.

4.4. Experiments vs. simulations

Although *MOBS* and *MOBO* controllers show almost 40% energy savings during the experiments, while simulation studies in [1] predicted energy savings between 45% and 55% depending on outside weather. The savings during the experiments are slightly lower than that of during the simulations because the currently used control logic used at the AHU in Pugh Hall is more efficient that the control logic used during the simulations. While the baseline controller in the simulation study did not use nighttime setback, the one currently used in Pugh Hall does. In particular, it closes the OA dampers supplying 100% return air during nighttime setback period. This reduces energy consumption since it takes more energy to condition hot and humid outside air than to condition return air.

Although the simulation study assumed that we have measurements of occupancy count, in the experiments we estimated the occupancy using a conservative approach: whenever the room was occupied, we assumed it was occupied by its maximum design occupancy. This estimation scheme was necessarily conservative during most times. The experimental results thus indicate that the control algorithm is robust to inaccuracies in occupancy measurement through such conservative measures. We conclude that for zones with small design occupancy, motion detectors or other means of presence detection can be profitably used for occupancy measurement.

5. Conclusion and future work

Experimental results from implementing two occupancy-based control algorithms in a single zone are reported. The goal of the controllers is to minimize energy consumption while maintaining thermal comfort and indoor air quality. The results obtained here are remarkably consistent with that from the simulation results in [1]. In particular, both the rule-based MOBS controller and the MPC-based MOBO controller led to large and similar reduction in energy use over baseline. These results verify our conclusion in the simulation study that a simple rule-based feedback control performs as well as much more complex MPC-based control when they use occupancy measurements for control. Without occupancy predictions, the MPC-controller can only do what a well-designed feedback controller will also do, that is, set back the zone temperature when the zone is unoccupied, but not too much so that it can be changed quickly when occupancy changes, and maintain a minimum airflow rate to ensure good IAQ. Since the cost of MPC implementation is considerably higher than that for a rule-based controller, the additional benefit of MPC is negligible.

Another useful result of the experimental verification is that for small zones such as offices, motion detection based occupancy estimation—in spite of its inherent inaccuracy—can be effectively used for occupancy based control with large energy savings. Determining occupancy for larger spaces will require sensors that go beyond detecting presence. A sensor that can measure the number of people (such as thermal image/array sensors and video-cameras with image processing algorithms), are likely candidates for such applications.

There are many ways to extend this wok in future. The control algorithms presented here are zone-level strategies in which only the SA temperature and flow rate at VAV boxes are manipulated while treating the RA ratio, and CA temperature at AHU as exogenous inputs. It is possible if all the four inputs, i.e., the SA temperature, SA flow rate, RA ratio, and CA temperature, are controlled, MPC may yield significant savings over rule-based control. Preliminary investigation in this direction is carried out in [27].

In this paper, we have compared the performance of the controllers through experiments only for one day. Since energy savings depend on outside weather and climate, a longer time-horizon experiment needs to be conducted to obtain a more robust estimate of the energy savings potential of the occupancy-based controllers. In fact, we have implemented the MOBS controller in several zones of the Pugh Hall for a week. The results of this test will be reported elsewhere [21].

Another question that needs to be explored is the payback period of occupancy based control technology. The MOBS controller requires minimal additional hardware, only an occupancy sensor. The cost of sensor node is approximately $215 [22]. A detailed study needs to be done to calculate the payback time period (that includes the cost of the sensor node, additional equipment, and labor for installation) and operational maintenance cost.

Acknowledgment

The authors gratefully acknowledge the following people without whose help this paper would not have been possible: (i) Prof. Herbert A. Ingley for many helpful discussions, (ii) Rahul Subramany for the design and development of the sensor nodes, (iii) Yashen Lin and Jonathan Brooks for help with the experiments, (iv) Physical Plant Division at UF, especially Skip Rockwell and Peder Winkel, for help with control implementation in Pugh Hall, and (v) Computing Network Services at UF, especially Matt Grover, for help in integrating the wireless sensor network with the UF intranet.

References

[1] Goyal S, Ingley H, Barooah P. Occupancy-based zone climate control for energy efficient buildings: complexity vs. performance. Appl Energy 2013;106:209–21.
[2] Siroky J, Oldewurtel F, Cigler J, Privara S. Experimental analysis of model predictive control for an energy efficient building heating system. Appl. Energy 2011;88:3079–87.
[3] Mossolly M, Ghalib K, Ghaddar N. Optimal control strategy for a multi-zone air conditioning system using a genetic algorithm. Energy 2009;34(1):58–66. http://dx.doi.org/10.1016/j.energy.2008.10.001.
[4] US EIA-Department of Energy. CBECS detailed Table; 2003.
[5] ASHRAE. ANSI/ASHRAE standard 62.1-2010: ventilation for acceptable air quality; 2010.
[6] Gruber M, Trschel A, Dalenbck J-O. Model-based controllers for indoor climate control in office buildings complexity and performance evaluation. Energy Buildings 2014;68(0):213–22. Part A.
[7] Lin Y, Middelkoop T, Barooah P. Issues in identification of control-oriented thermal models of zones in multi-zone buildings. In: IEEE conference on decision and control; 2012. p. 6932–7. doi: http://dx.doi.org/10.1109/CDC.2012.6425958.
[8] Prívara S, Cigler J, Va Z, Oldewurtel F, Sagerschnig C, ekov E. Building modeling as a crucial part for building predictive control. Energy Buildings 2013;56(0):8–22. http://dx.doi.org/10.1016/j.enbuild.2012.10.024.
[9] Dong B, Lam K. A real-time model predictive control for building heating and cooling systems based on the occupancy behavior pattern detection and local weather forecasting. Build. Simul. 2014;7(1):89–106. http://dx.doi.org/10.1007/s12273-013-0142-7.
[10] Aswani A, Master N, Taneja J, Culler D, Tomlin C. Reducing transient and steady state electricity consumption in HVAC using learning-based model-predictive control. Proc. IEEE 2012;100(1):240–53.
[11] Patarello G. Model predictive control of HVAC systems: design and implementation on a real case study [Master's thesis]. University of Padua, Padua, Italy; 2013.

[12] Bengea SC, Kelman AD, Borrelli F, Taylor R, Narayanan S. Implementation of model predictive control for an HVAC system in a mid-size commercial building. HVAC&R Res 2013;20:121–35.
[13] Agarwal Y, Balaji B, Dutta S, Gupta R, Weng T. Duty-cycling buildings aggressively: the next frontier in HVAC control. In: Information processing in sensor networks (IPSN); 2011. p. 246–57.
[14] Balaji B, Xu J, Nwokafor A, Gupta R, Agarwal Y. Sentinel: occupancy based HVAC actuation using existing WiFi infrastructure within commercial buildings. In: Proceedings of the 11th ACM conference on embedded networked sensor systems, SenSys '13. New York, NY, USA: ACM; 2013. p. 17:1–17:14. http://dx.doi.org/10.1145/2517351.2517370.
[15] Gao PX, Keshav S. SPOT: a smart personalized office thermal control system. In: Proceedings of the fourth international conference on future energy systems, e-Energy '13. New York, NY, USA: ACM; 2013. p. 237–46. http://dx.doi.org/10.1145/2487166.2487193.
[16] Padmanabh K, Malikarjuna VA, Sen S, Katru SP, Kumar A, et al. iSense: a wireless sensor network based conference room management system. In: Proceedings of the first ACM workshop on embedded sensing systems for energy-efficiency in buildings, BuildSys '09. New York, NY, USA: ACM; 2009. p. 37–42. http://dx.doi.org/10.1145/1810279.1810288.
[17] Erickson VL, Achleitner S, Cerpa AE. POEM: power-efficient occupancy-based energy management system. In: Proceedings of the 12th international conference on information processing in sensor networks, IPSN '13. New York, NY, USA: ACM; 2013. p. 203–16. http://dx.doi.org/10.1145/2461381.2461407.
[18] ASHRAE. ANSI/ASHRAE standard 55-2010. Thermal environmental conditions for human occupancy; 2010.
[19] Goyal S, Barooah P. A method for model-reduction of nonlinear building thermal dynamics of multi-zone buildings. Energy Buildings 2012;47:332–40.
[20] ASHRAE. The ASHRAE handbook – HVAC applications. SI ed.; 2011.
[21] Brooks J, Goyal S, Subramany R, Lin Y, Middelkoop T, Arpan L, Carloni L, Barooah P. An experimental investigation of occupancy-based energy-efficient control of commercial building indoor climate. In: IEEE CDC; 2014. <http://humdoi.mae.ufl.edu/pbarooah/PBpublication.html> (accepted).
[22] Subramany R. Wireless sensor network for HVAC control [Master's thesis]. University of Florida; 2013.
[23] Wächter A, Biegler L. On the implementation of an interior-point filter line-search algorithm for large-scale nonlinear programming. Math. Program. 2006;106:25–57.
[24] Middelkoop T. High-resolution data collection for automated fault diagnostics. In: Capehart BL, Brambley M, editors. Automated diagnostics. Atlanta, GA: Fairmont Press; September, 2014.
[25] University of Florida Department of Physics weather station. <http://www.phys.ufl.edu/weather/>.
[26] ASHRAE. The ASHRAE handbook fundamentals. SI ed.; 2005.
[27] Goyal S, Barooah P. Energy-efficient control of an air handling unit for a single-zone VAV system. In: IEEE conference on decision and control; 2013: p. 4796–801. doi: http://dx.doi.org/10.1109/CDC.2013.6760641.